Numerical Analysis of the Vertical Instability Stabilizing Effect of Saddle Coils in Tokamak*)

Shin NAITO, Yasuhiro SUZUKI[1)] and Hiroaki TSUTSUI[2)]

School of Environment and Society, Department of Transdisciplinary Science and Engineering, Tokyo Institute of Technology, Ookayama 152-8550, Japan

[1)]*Graduate School of Advanced Science and Engineering, Hiroshima University, Kagamiyama 739-8511, Japan*

[2)]*Institute of Innovative Research, Tokyo Institute of Technology, Ookayama 152-8550, Japan*

(Received 12 January 2022 / Accepted 13 March 2022)

The stabilizing effect of tokamak plasma vertical position with saddle coils, which had been experimentally confirmed on the small tokamak PHiX, is evaluated numerically. The growth rate of the vertical position instability was evaluated by the three-dimensional linearized ideal MHD stability analysis code TERPSICHORE. The results of the evaluation showed that the growth rate decreased (increased) when the saddle coils were excited in the normal (inverted) direction, where the plasma vertical position had been stabilized (destabilized) in the experiments. It was also found that the growth rate was inversely proportional to the square of the saddle coils current, which was consistent with the tendency obtained experimentally. These results show that the TERPSICHORE code qualitatively reproduces the stabilizing effect of saddle coils.

Keywords: tokamak, vertical stability, saddle coil, non-axisymmetric equilibria, magnetohydrodynamic stability, TERPSICHORE

DOI: 10.1585/pfr.17.2403069

1. Introduction

It is well known that increasing the elongation ratio κ of tokamak plasma can improve the toroidal β limit [1, 2] and the energy confinement time [3]. On the other hand, increasing κ causes the instability of the plasma vertical position. To keep the position of unstable plasma, feedback control of the plasma position and the installation of conducting walls near the plasma is often applied. In addition to the above methods, the vertical position can be stabilized by applying a non-axisymmetric magnetic field generated by continuously wound helical coils. This phenomenon has been studied both theoretically [4] and experimentally [5, 6]. It has also been experimentally found that the vertical position can be stabilized by using semi-stellarator windings, which are helical coils installed only outside of the torus [7], and local coils [8].

We have succeeded in stabilizing the vertical position of plasma by using saddle coils with simple shapes which do not go through the inside of the torus [9]. Figure 1 shows the arrangement of the saddle coils and the $|B|$ distribution on of the Last Closed Flux Surface (LCFS). The saddle coils consist of eight small coils on the top and bottom, and two side coils on the outer sides of the torus. By exciting each of these ten coils in the direction shown in Fig. 1, non-axisymmetric magnetic fields with the toroidal periodicity $M = 1$ are generated. Those magnetic fields produce the plasma vertical position stabilizing effect. Also, those magnetic fields cause to a non-axisymmetric deformation of the tokamak plasma. In Ref. [9], we calculated horizontal field B_r^{ave} by the magnetic field lines tracing [10], and numerically investigated the stabilizing effect of the field on the plasma vertical position. By using only B_r^{ave}, however, we could not conduct the quantitative stability analysis numerically, even though we could confirm the existence of a magnetic field structure which stabilizes the vertical position. To quantitatively evaluate

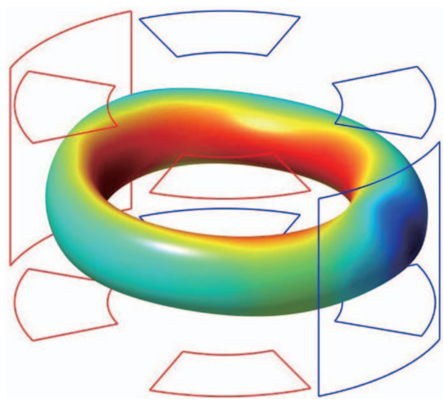

Fig. 1 Arrangement of saddle coils and the $|B|$ distribution on the last closed flux surface. The colors of saddle coils indicate the direction of current.

author's e-mail: naito.shin@torus.nr.titech.ac.jp

*) This article is based on the presentation at the 30th International Toki Conference on Plasma and Fusion Research (ITC30).

the stabilizing effect of saddle coils, the stability analysis was performed with the three-dimensional linearized ideal MHD stability analysis code TERPSICHORE.

Following this introduction, the details of the TERPSICHORE code are described in Section 2. The three-dimensional equilibria used as input for the MHD stability analysis are shown in Section 3. The results of the stability analysis of the plasma vertical position calculated by the TERPSICHORE are shown in Section 4. The summary is provided in Section 5.

2. TERPSICHORE Code

The TERPSICHORE code solves the following linearized ideal MHD equation in variational form for three-dimensional equilibria [11],

$$\omega^2 \delta W_{\mathrm{k}} = \delta W_{\mathrm{p}} + \delta W_{\mathrm{v}}, \tag{1}$$

where $\omega^2 \delta W_{\mathrm{k}}$ is the perturbed plasma kinetic energy, δW_{p} is the perturbed plasma potential energy, and δW_{v} is the perturbed magnetic energy of the space between the plasma and the conducting wall. The eigenvalue ω^2 means the perturbed mode is stable when $\omega^2 > 0$. The perturbed displacement vector ξ is defined in Boozer coordinate as

$$\xi = \sqrt{g}\xi^s \nabla\theta \times \nabla\phi + \eta(\mathbf{B} \times \nabla s / B^2). \tag{2}$$

Here, s, θ, and ϕ are the radial component, poloidal and toroidal angles in Boozer coordinate. The Jacobian $\sqrt{g}$ is proportional to $1/B^2$. The radial and magnetic surface components of ξ are ξ^s and η, respectively. Both components are represented as sums of Fourier series:

$$\xi^s(s,\theta,\phi) = \sum \xi_l(s) \sin(m_l\theta - n_l\phi + \varDelta), \tag{3}$$

$$\eta(s,\theta,\phi) = \sum \eta_l(s) \cos(m_l\theta - n_l\phi + \varDelta), \tag{4}$$

where l is an index of poloidal and toroidal mode number pair (m_l, n_l), and $\varDelta$ is an arbitrary phase factor. It should be noted that ξ of Eq. 2 is chosen to eliminate the component parallel to $\mathbf{B}$.

The TERPSICHORE code calculates eigenvalues and mode structures of selected Fourier mode pairs of ξ. Analyzing the stability of vertical position in the TERPSICHORE, $n = 0$ modes called "axisymmetric mode" or "vertical mode" were selected for calculations. The stability analyses under such conditions have been performed for NCSX [12], and DIII-D with non-axisymmetric coils [13]. In this paper, $m_l = 1$ - 20, $n_l = 0$, a total of 20 axisymmetric mode pairs were selected and the vertical positional stability was evaluated by their eigenvalues (growth rates).

3. Input 3D Equilibrium

The TERPSICHORE code uses the equilibrium calculated with the three-dimensional equilibrium calculation code VMEC [14]. In this section, we show the equilibrium used for the input of the TERPSICHORE code. We adopted the same coil geometry as the small tokamak device PHiX and calculated the equilibrium with saddle coils

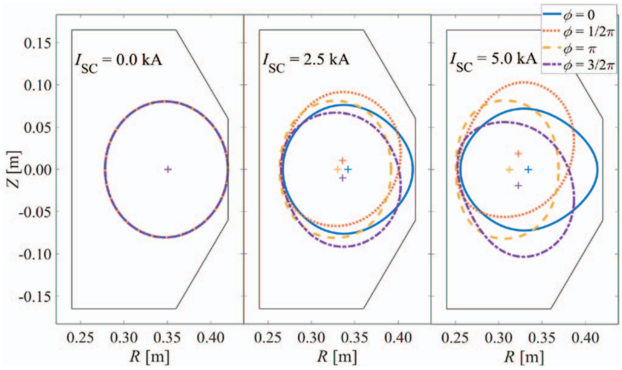

Fig. 2 LCFS with $I_{\mathrm{SC}} = 0.0$ kA (left), $I_{\mathrm{SC}} = 2.5$ kA (middle), $I_{\mathrm{SC}} = 5.0$ kA (right). Makers of "+" and black hexagon indicate the positions of magnetic axes and the limiter of PHiX, respectively.

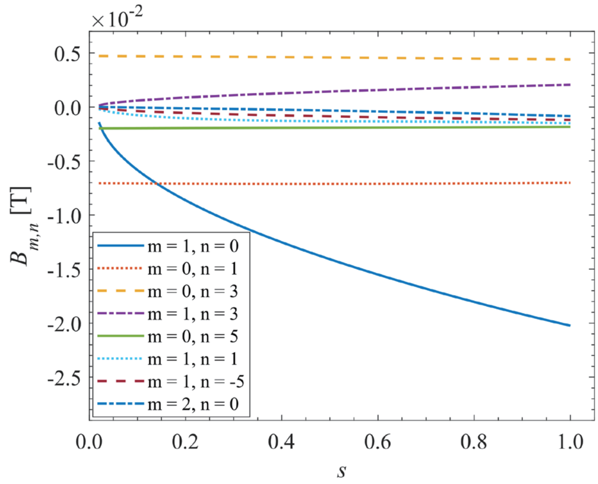

Fig. 3 Boozer spectrum of the equilibrium with $I_{\mathrm{SC}} = 5.0$ kA. The Fourier mode of B_{00} is excluded.

current $I_{\mathrm{SC}} = 0.0$ - 5.0 kA. The conditions applied to the VMEC code calculations are as follows: All the equilibria were fixed to the plasma current $I_{\mathrm{p}} = 2.5$ kA, the number of calculated magnetic surfaces $N_{\mathrm{s}} = 101$, the toroidal flux of the plasma $\varPhi = 1.55 \times 10^{-3}$ Wb, and the LCFS was in touch with the outer side of the limiter of PHiX. The numbers of Fourier modes in toroidal and poloidal directions used for representing flux surfaces were $0 \le m \le 3$ and $-16 \le n \le 16$, respectively. The value of n was taken up to the higher-order accounting for the ripples of the 16 toroidal field coils. The plasma current density profile j was assumed to be parabolic, $j = j_0 + j_1 s_{\mathrm{f}}^2$, where s_{f} was the normalized toroidal flux, j_0 and j_1 were coefficients of the current density. We also assumed zero-β in all equilibria. It is emphasized that the axisymmetric magnetic fields are different on each calculated equilibrium. This is due to the adjustment of effective vertical magnetic fields generated by the saddle coils.

Figure 2 shows the LCFS of the calculated equilibrium with $I_{\mathrm{SC}} = 0.0$, 2.5, and 5.0 kA. The LCFS is elon-

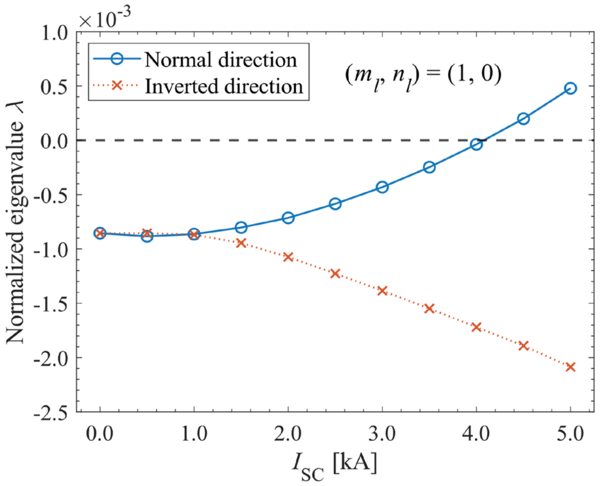

Fig. 4 Normalized eigenvalue versus I_{SC}. Makers of “o” and “x” indicate λ of the saddle coils current in normal direction and inverted direction, respectively.

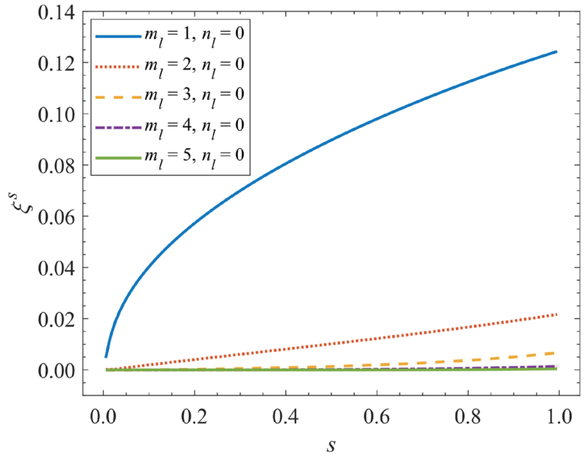

Fig. 5 Mode structures of radial displacement vector at I_{SC} = 5.0 kA.

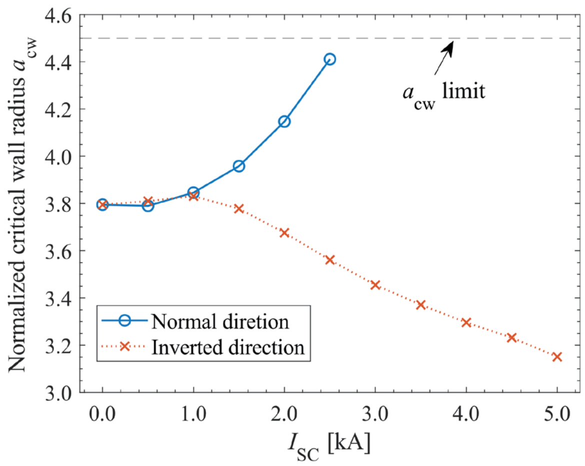

Fig. 6 Normalized critical wall radius a a_{cw} versus I_{SC}. Makers of “o” and “x” indicate a a_{cw} of the saddle coils current in normal direction and inverted direction, respectively.

gated on toroidal average in all conditions due to the quadrupole magnetic field component of the axisymmetric coils. Under the condition of I_{SC} = 0.0 kA, the elongation ratio is κ = 1.15. As I_{SC} increases, the non-axisymmetry of the flux surfaces becomes stronger and the magnetic axes rotate, closer to a Heliac stellarator-like equilibrium. To investigate the magnetic field structure of the plasma with the magnetic field generated by the saddle coils, the Boozer spectrum of the equilibrium with I_{SC} = 5.0 kA was calculated using the BOOZ_XFORM code [15]. As shown in Fig. 3, a toroidicity component $(m, n) = (1, 0)$ was the highest amplitude component, similar to the axisymmetric tokamak. The $n \neq 0$ non-axisymmetric components are, however, increasing with considerable intensity. Those components are generated by the saddle coils. Furthermore, compared with the experimental results in Ref. [9], it is presumed that those components contribute to the stabilization of the plasma vertical position.

4. Results of the Stability Analysis

The stability analysis of the plasma vertical position was performed by the TERPSICHORE code to calculate the normalized eigenvalue $\lambda = \omega^2/\omega_A{}^2$. It should be noted that the discussion on the absolute value of λ is provided in the following references [16]. Here, ω_A is the Alfvén frequency. In the stability analysis of the TERPSICHORE code, the ideal conducting walls with finite radius must be set. In order to minimize the effect of the conducting walls and investigate only the stabilizing effect of the saddle coils, axisymmetric walls (wall major radius R_w = 0.33 m, wall minor radius a_w = 0.32 m, wall ellipticity κ_w = 1.8) were set up to place the wall as far away from the plasma as possible. It is almost impossible to make the a_w larger since the conducting walls cross the center of the torus.

Figure 4 shows the calculated λ versus the saddle coil current I_{SC}. The value of λ is that of the $(m_l, n_l) = (1, 0)$ mode which is the most unstable in the chosen modes of ξ.

By inverting the energizing direction of the two saddle coils located on the sides of the torus, the averaged horizontal magnetic field $B_r{}^{ave}$ can be reversed (inverted direction). The result of λ with inverted direction is also shown in Fig. 4 as well as the λ with the normal direction shown in Fig. 1. We observe that λ is monotonically increasing in I_{SC} with normal direction though monotonically decreasing in I_{SC} with inverted direction. The experimental results also showed that the vertical position of the plasma was stabilized (destabilized) in the I_{SC} with normal direction (inverted direction) (see Fig. 6 in Ref. [9]). This demonstrates that the TERPSICHORE code reproduces the vertical position stabilizing (destabilizing) effect of the saddle coils which had been confirmed experimentally. In addition, it is found that λ becomes zero at $I_{SC} \sim$ 4.0 kA with normal direction. It means that the equilibrium of

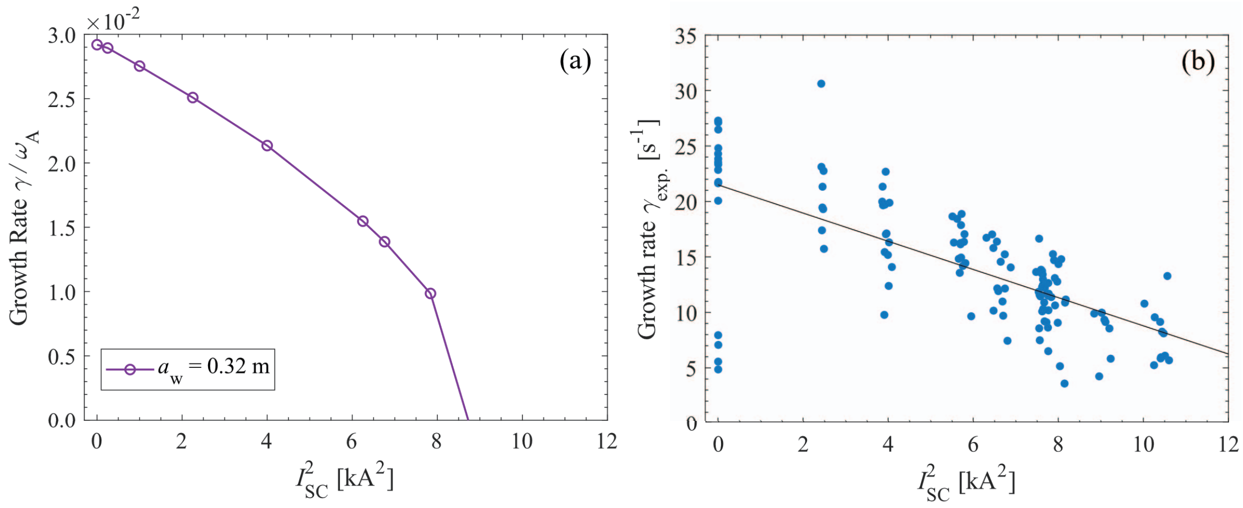

Fig. 7 Comparison between the growth rate calculated by TERPSICHORE (a) and the growth rate obtained experimentally (b). The line in Fig. 7 (b) is the result of a linear fitting.

$\kappa = 1.15$ is vertically stabilized without conducting walls when $I_{SC} > 4.0$ kA.

We also calculated the radial component ξ^s of the displacement vector ξ, under the same conditions as in Fig. 4. Figure 5 shows the result at $I_{SC} = 5.0$ kA, only the five most dominant modes are shown. The mode structures are almost the same over all of I_{SC} conditions. The most dominant mode for all I_{SC} is $(m_l, n_l) = (1, 0)$ as mentioned above, which represents the rigid body displacement when the plasma shifts vertically.

Since the effect of the conducting walls on λ cannot be completely excluded, the plasma vertical position stabilizing effect of the saddle coils was also evaluated as the wall minor radius required for the stabilization. The walls were set to be non-axisymmetric to match the plasma shape, and the normalized critical wall radius $a_{cw} = a_w/a_p$ at the value of $\lambda \sim 0$ was defined as the wall minor radius required for stabilization. Here a_p is the averaged plasma minor radius. In addition, the non-axisymmetric walls were produced by multiplying by a factor of $m \neq 0$ Fourier components of the input VMEC equilibria. Figure 6 shows the a_{cw} versus I_{SC}. Since the a_{cw} reached its maximum value around $a_{cw} \sim 4.5$ and could not be increased any further, the values of a_{cw} for $I_{SC} > 3.0$ kA with normal direction were not calculated. The tendency of a_{cw} is similar to that of λ in Fig. 4. Compared to $I_{SC} = 0.0$ kA, a_{cw} increases by 16% with normal direction and decreases by 6% with inverted direction when $I_{SC} = 2.5$ kA. The reason for the different rates of change in a_{cw} at equilibrium for the different directions is unclear. It may be due to the difference in the shape of the flux surfaces at each condition.

We compared the experimental growth rate $\gamma_{exp.}$ with the normalized growth rate γ/ω_A calculated by the TERPSICHORE code. The growth rate γ is defined as $\gamma^2 = -\omega^2$. The values of $\gamma_{exp.}$ were calculated from the experimental results which is the relationship between vertical drift speed and I^2_{SC} of Fig. 9 (a) in Ref. [9]. Both the plasma condition when measuring $\gamma_{exp.}$ and the details of the measurement are explained in Ref. [9]. The axisymmetric magnetic field in the VMEC code calculation has been changed to the dipole magnetic field to bring the equilibrium closer to those of the experiments. The rest of the calculation conditions were identical to those described in section 2. In addition, the conducting walls required for the calculation of the TERPSICHORE code were set to the same axisymmetric walls used in the results of Figs. 4, 5. We emphasize that the equilibrium used in Fig. 7, however, is not the equilibrium obtained by the flux surfaces reconstruction. In Fig. 7 (b), $\gamma_{exp.}$ shows a linear and inversely proportional decreasing tendency with I^2_{SC}, and the same tendency is observed for γ/ω_A in Fig. 7 (a). Though it can be seen that the linearity of γ/ω_A worsens around I^2_{SC} $\sim$6 kA^2 in Fig. 7 (a), the behavior is caused by what the TERPSICHORE code cannot evaluate the small value of γ accurately. It should be noted that we did not compare absolute values of growth rates. This is because the TERPSICHORE code cannot include non-linear effects, and the growth rate of the TERPSICHORE code was obtained at the plasma vertical position $Z_p = 0$, while the experimental growth rate was obtained at $Z_p \neq 0$. From the results shown in Fig. 7, it is experimentally and numerically confirmed that the plasma vertical position stabilizing effect of the saddle coils increases in proportion to I^2_{SC}.

The phenomenon confirmed above can be explained by the following expression: The field line averaged magnetic field B_{ave} generated by the helical coils is proportional to $B_{ave} \approx {I_s}^2/B_t$ [7]. Here, I_s is the current of the helical coils, B_t is the toroidal field. Since a force of $j \times B_{ave}$ affects the plasma and contributes to the stabilization of the plasma vertical position, the growth rate of the vertical displacement is inversely proportional to I^2_{SC} in the same way.

5. Summary

In this paper, we used the three-dimensional linearized ideal MHD stability analysis code TERPSICHORE to evaluate the stabilizing (destabilizing) effect of the plasma vertical position of the saddle coils. As a result, the relationship between the eigenvalue (growth rate) calculated by the code and the saddle coils current was consistent with the tendency obtained in the experiments. Hence, it is confirmed that the TERPSICHORE code can qualitatively reproduce the stabilizing (destabilizing) effect of the saddle coils. In addition, the stabilization effect was quantitatively evaluated from the eigenvalues and normalized minor conducting wall radius. Furthermore, the properties of the three-dimensional equilibrium calculated by the VMEC code used as input was discussed.

Now that the results in this manuscript imply that the TERPSICHORE code will be useful to design new coils, it may be possible to design new coils with a higher stability effect, by using the eigenvalues calculated by the code as the input of the target function. We will design such new coils in the future.

Acknowledgements

The authors would like to express their gratitude to Dr. W.A. Cooper for his advice regarding the TERPSICHORE code. This work is performed with the support of the Grant-in-Aid for JSPS Fellows (21J10404), JSPS KAKENHI (21H01061) and the NIFS Collaboration Research program (NIFS18KOAP033).

[1] E.J. Strait, Phys. Plasmas **1**, 1415 (1994).
[2] F. Troyon *et al.*, Plasma Phys. Control. Fusion **26**, 209 (1984).
[3] P.N. Yushmanov *et al.*, Nucl. Fusion **30**, 1999 (1990).
[4] G.Y. Fu, Phys. Plasmas **7**, 1079 (2000).
[5] K. Sakurai and S. Tanahashi, J. Phys. Soc. Jpn. **49**, 759 (1980).
[6] M.C. ArchMiller *et al.*, Phys. Plasmas **21**, 056113 (2014).
[7] H. Ikezi, K.F. Schwarzenegger and C. Ludescher, Phys. Fluids **22**, 2009 (1979).
[8] K. Yasuda *et al.*, Phys. Plasmas **28**, 082108 (2021).
[9] S. Naito *et al.*, Nucl. Fusion **61**, 116035 (2021).
[10] K. Yasuda *et al.*, Plasma Fusion Res. **15**, 1402083 (2020).
[11] D.V. Anderson *et al.*, Int. J. Supercomput. Appl. **4**, 34 (1990).
[12] G.Y. Fu *et al.*, Fusion Sci. Technol. **51**, 218 (2007).
[13] A.D. Turnbull *et al.*, Nucl. Fusion **56**, 086006 (2016).
[14] S.P. Hirshman, W.I. van Rij and P. Merkel, Comput. Phys. Commun. **43**, 143 (1986).
[15] R. Sanchez *et al.*, Plasma Phys. Control. Fusion **42**, 641 (2000).
[16] A.D. Turnbull, W.A. Cooper, L.L. Lao and L.P. Ku, Nucl. Fusion **51**, 123011 (2011).